Current Applied Science and Technology Vol. 23 No. 1 (January-February 2023)

Research article

Assessment of Hydrocarbon Pollution in Groundwater Using Electrical Resistivity Method

Lukumon Adeoti, Geraldine Chibuzor Anukwu*, Adeola Saheed Ademoye, Joseph Taye Adegbite, Oluwakemi Adeogun and Emmanuel Olutayo Adigun

Department of Geosciences, University of Lagos, Akoka, Nigeria

Received: 20 December 2021, Revised: 17 April 2022, Accepted: 29 April 2022

DOI: 10.55003/cast.2022.01.23.003

Keywords

leakages;
contamination;
geoelectric sections;
longitudinal conductance ;
aquifer;
pipeline;
groundwater system

Abstract

Hydrocarbon contamination of the groundwater system is a problem facing residents of Ejigbo, Lagos, Southwestern Nigeria. The area hosts the busiest satellite petroleum depots in Nigeria, and residents have attributed pollution of the groundwater system to hydrocarbon spills from possible pipeline leakages. This study aimed to identify and characterize the source and extent of the groundwater system contamination in the study area. The electrical resistivity method was adopted, comprising 2D Electrical resistivity imaging (ERI) and Vertical Electric Sounding (VES) techniques. Data acquired were processed and analyzed to obtain geoelectric sections, longitudinal conductance map and 2D ERI sections for the study area. Three distinct geoelectric zones were delineated, with the intermediate zone identified as the contaminated shallow aquiferous unit. This unit's resistivity values ranged from about 400 - 5000 ohm-m at a depth of 5 - 35 m. On the 2D ERI sections, possible locations of pipeline leakages were identified. On some ERI sections, a linear feature with resistivity value less than 300 ohm-m was observed from the surface down the depth of the entire section, truncating the horizontal flow of the contaminated unit. Generally, the results indicate that the contamination of the shallow aquifer in the area is widespread and mitigation measures should be urgently undertaken.

1. Introduction

Water is an essential resource for the sustenance of life on earth. Demand for potable water has increased over the years due to population growth, industrialization and agricultural activities. This increase poses a challenge to the availability, quality and sustainability of the resource. A major source of potable water for about one-third of the world's population is groundwater due to its

*Corresponding author: Tel.: (+234) 905 638 6645
E-mail: ganukwu@unilag.edu.ng

reliability, availability and accessibility [1]. However, there has been a growing concern over groundwater pollution in recent times, especially as a result of hydrocarbon exploration, exploitation and use. The release of hydrocarbon plumes into the groundwater system is a global issue that has been occurring since the discovery of crude oil. It often happens due to poor production operation, corrosion and vandalization of pipelines [2]. The consequence of this is the reduction in the quality of the groundwater system within the polluted environment, making the water unsafe for consumption and also posing health risks [3]. Therefore, adequate steps must be taken to guarantee the integrity of the groundwater resource.

Characterization of the hydrocarbon pollution of groundwater is a significant step towards mitigating the effect of such contamination. Various techniques are available for characterizing hydrocarbon pollution; however, the geophysical methods provide a fast and cost-effective means of undertaking such investigations. More specifically, the electrical resistivity method has been successfully utilized in the mapping of groundwater contamination as well as in the investigation of aquifer protective capacity [4, 5]. The technique measures the electrical resistivity of the subsurface materials. Electrical resistivity of subsurface materials is a function of several soil properties such as porosity, hydraulic permeability, moisture content, concentration of dissolved electrolytes and temperature. In characterizing subsurface contaminated zones, the resistivity contrast between contaminated and uncontaminated zones provides a means by which the geometry and flow direction of the contaminant is mapped. The resistivity signature associated with oil spillage is typically indicated by the presence of a high resistivity anomaly as hydrocarbons tend to have higher resistivities compared to water [6, 7]. However, several researchers have also reported the presence of low resistivity anomalies associated with hydrocarbon contamination [8, 9]. Such low resistivity anomaly has been attributed to the presence of inorganic compounds and/or biodegradation of the hydrocarbons.

An important factor that also determines the contamination of the groundwater system is the protective capacity. Groundwater in aquifers whose overburden layers have low protective capacity is highly vulnerable to surface contamination from various sources such as landfills, septic systems and oil spills [10]. The vulnerability of an aquifer can be determined from its Dar Zarrouk parameters (Longitudinal conductance and Transverse resistance), which are employed in aquifer protection studies and in the evaluation of hydrologic properties [11, 12].

Ejigbo town is located in Lagos State, Southwestern Nigeria. It has a population of more than 50,000 and hosts one of the busiest satellite petroleum depots of the Nigerian National Petroleum Corporation (NNPC). The depot, which accounts for about 60% of fuel supply in Nigeria, has become a source of agony to inhabitants of the community due to reported leaking petroleum pipes. The shallow wells and boreholes dug by the residents constitute the primary source of potable water for this area. However, over the years, there have been reports of contamination of the groundwater system by hydrocarbon products (Figure 1) [13]. Therefore, this present study aimed

Figure 1. Fuel water from tap (left) and an abandoned hand dug well (right) in Ejigbo, Lagos [13].

to determine the location of the hydrocarbon leakages and the extent of the pollution in the groundwater system in the Ejigbo area of Lagos State, Nigeria.

The study area is located in Ejigbo, a suburb of Lagos State, Southwestern Nigeria and has an average elevation of about 35m above sea level. Ejigbo is a predominantly residential area with an approximate population of 50,000 inhabitants. Two distinct geologies cover Nigeria, the basement complex and the sedimentary basin. Lagos state falls under the sedimentary basin; in particular, it is within the Southwestern Nigerian sector of the Dahomey Basin [14]. The study area falls under the coastal plain sands geology of Lagos State (Figure 2a). The coastal plain sands, amongst other aquiferous units, are the most exploited and utilized water-bearing strata in Lagos [15]. The aquifer depth ranges from ground level to less than 200 m [16].

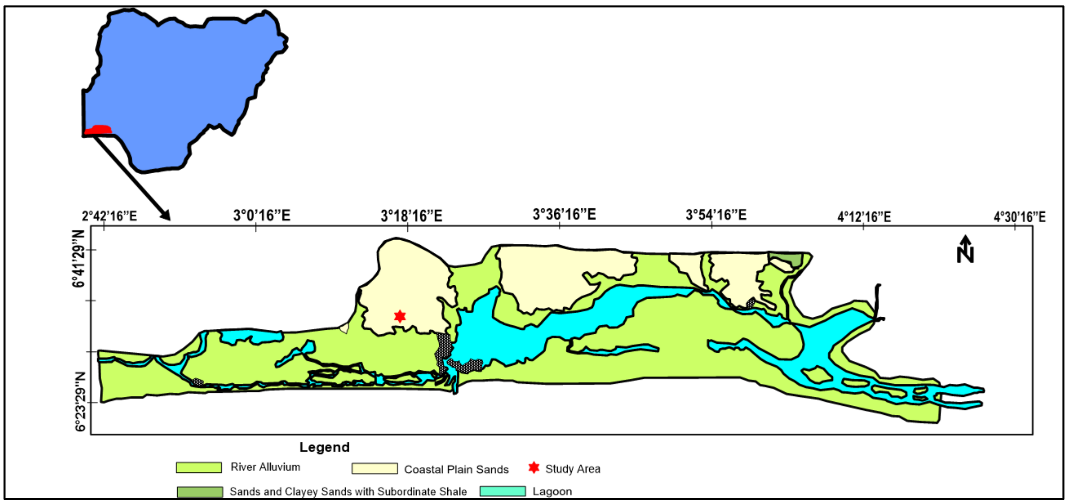

Figure 2. Geological map of Lagos State Nigerian sector [17], with an inset of the Map of Nigeria showing the location of Lagos

2. Materials and Methods

2.1 Data acquisition

2D Electrical Resistivity Imaging (ERI) measurements were conducted along seven traverses in the study area (Figure 3) and two traverses at locations known to be free from hydrocarbon contamination. In all, space availability, accessibility and pipeline orientation were considered prior to establishing the traverses. The data were acquired using a PASI terrameter while deploying the Wenner electrode configuration. The 2D measurements were conducted as a series of 1D (four electrodes) measurements along the survey area, with a minimum electrode spacing (a) of 10 m for all traverses, except for traverse 3 (a = 5 m). Subsequently, the spacing was increased to 2a, 3a, 4a, 5a and 6a, respectively. The spread of the traverses ranged from 100-200 m. Electrode spacing for the 2D measurements was chosen, factoring in the ability to resolve the shallow aquifer unit estimated to occur at a depth of about 3-13 m [16], available space at the site, and ease of data acquisition since the 2D measurements were not automated.

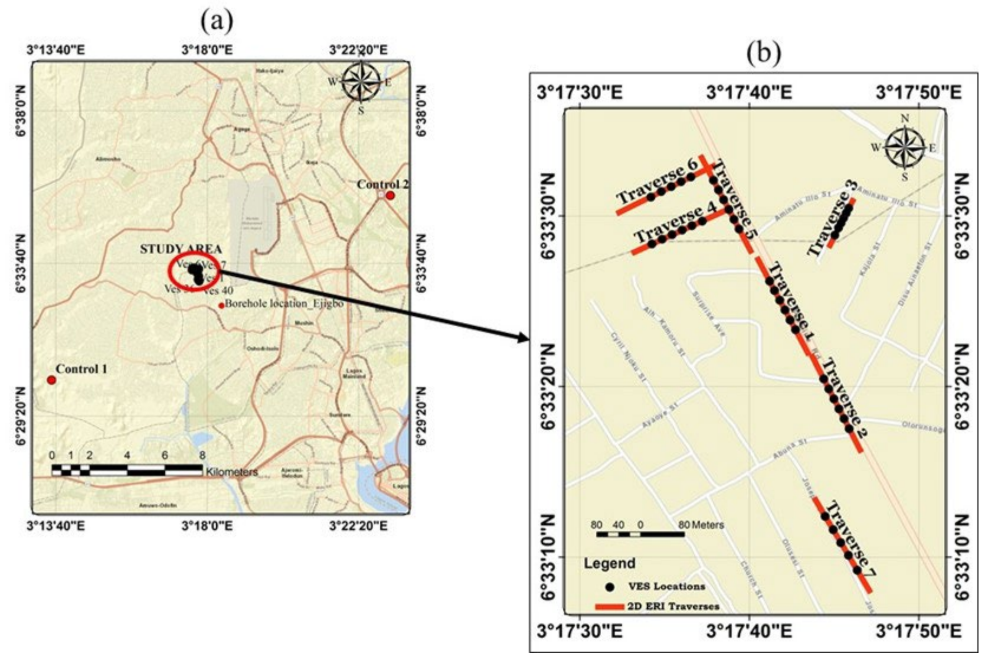

Figure 3. (a) Location of the study area and the control points within Lagos, southwestern, Nigeria (b) Shows the 2D ERI traverses and VES locations

Also, Vertical Electrical Resistivity Sounding (VES) measurements using the Schlumberger configuration were acquired at forty (40) locations at different points along the seven traverses in the study area (Figure 3) using the same instrument. The electrode spacing, AB/2, varied from a minimum of 1 m to a maximum of 250 m.

2.2 Data processing

Analysis of the 2D ERI data was carried out using the RE2DINV software [18]. The software produces a 2D resistivity model of the subsurface by computing the apparent resistivity values from the measurements obtained. An inversion is then implemented using the non-linear least-squares optimization technique [19]. For this study, the finite element subroutine was utilized for the forward modeling and the smoothness constrained least square method for the inversion. The result is a set of apparent resistivity, pseudo-section and inverted resistivity section for each traverse. For each case, the accepted subsurface model had no significant change between subsequent iterations [20]. Furthermore, the accepted earth model was also constrained by the interpretation obtained from the 1-D VES [21].

For the VES analysis, the data were plotted as curves and interpreted quantitatively using the partial curve matching technique with a two layer master curve and auxiliary curves. Subsequently, the geoelectric parameters (layer resistivity and thickness) obtained from the partial curve matching were then used as starting model for computer-based inversion using the IPI2Win software. The geoelectric parameters obtained from the inversion of the curves for all VES points along each traverse were used to generate geoelectric sections. Borehole log obtained at a location close to the study area (Figure 4), and the geology of the study area were used to aid the interpretation of the results and infer the subsurface lithology.

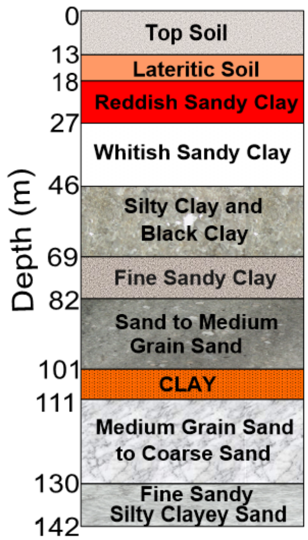

Figure 4. Borehole log at a location in NNPC Ejigbo

2.3 Longitudinal conductance and protective capacity

The first order geo-electric parameters (apparent resistivity and thickness of the layers above the aquifer) obtained from the analysis of the VES data for each location were used in deriving the total longitudinal conductance (Equation 1). The longitudinal conductance provides a means by which the impermeability of a layer can be measured [22].

$$S_L = \sum_{i=1}^{n} \frac{h_i}{\rho_i} \tag{1}$$

Where: ρ is the layer resistivity in Ωm.
h is the layer thickness in m.
SL is the longitudinal conductance in mhos.
i = 1, 2, 3, … nth layer.

The total longitudinal conductance values were then correlated to the protective capacitance of the aquifers and vulnerability, as shown in Table 1.

Table 1. Protective capacity rating

S_L (mho)	Protective capacity rating [23]	Vulnerability [24]
>10	Excellent	Extremely low vulnerability
5–10	Very good	Low vulnerability
0.7–4.9	Good	Moderate vulnerability
0.2–0.69	Moderate	High vulnerability
<0.19	Weak/Poor	Extremely high vulnerability

3. Results and Discussion

3.1 Vertical Electrical Sounding (VES)

The apparent resistivity curves obtained for some VES locations in the study area are shown in Figure 5. An analysis of the curves indicates the presence of different curve types in the area, with the AK curve usually predominant (Figure 6). Generally, the K-curve, which implies an intermediate layer with higher resistivity, is present in curves. The model parameters obtained from the inversion of the apparent resistivity curves are presented in Table 2.

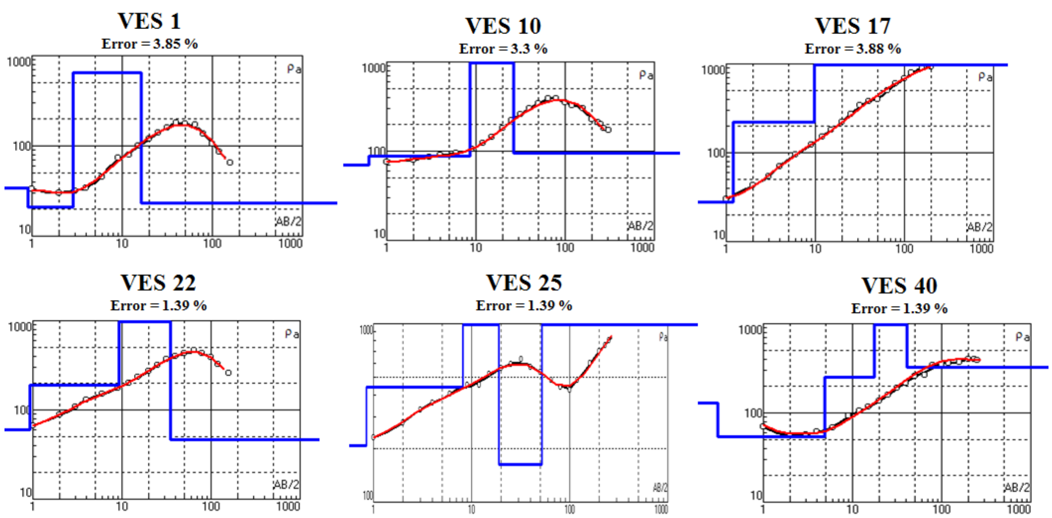

Figure 5. VES curves obtained from selected stations, showing the inverted resistivity model curve obtained and error

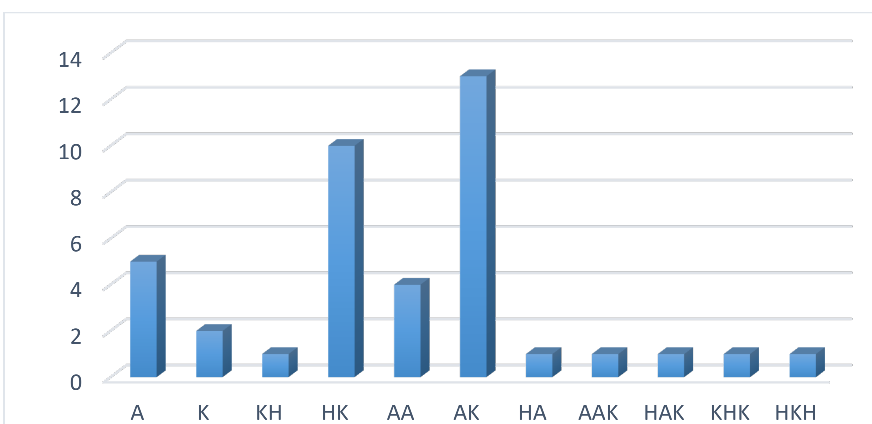

Figure 6. Graph showing VES curve types in the area

Table 2. Geoelectric parameters obtained from the analysis of the VES measurements

VES Location	Resistivity (ohm-m)						Depth (m)					Longitudinal Conductance
	ρ1	ρ2	ρ3	ρ4	ρ5	ρ6	h1	h2	h3	h4	h5	(mho)
1	34.1	21.1	644.0	23.0			0.9	2.0	13.2			0.14
2	104.0	10.0	54.0	842.0	15.8	1545.0	0.4	0.5	2.8	5.5	19.4	1.34
3	54.9	19.4	736.0	71.7			1.5	1.8	5.8			0.13
4	52.6	877.0	71.6				5.7	7.8				0.12
5	47.3	1021.0	16.3	1506.0			4.6	4.1	23.6			1.55
6	22.4	63.9	586.0	47.7			0.1	5.5	16.3			0.12
7	216.0	46.3	1756.0	151.0			1.1	3.2	7.6			0.08
8	15.5	49.6	1705.0	99.8			0.2	4.7	7.7			0.11
9	135.0	41.3	1668.0	79.4			1.3	1.6	17.1			0.06
10	70.6	88.6	1711.0	95.0			0.6	8.0	17.9			0.11
11	86.4	408.0	99.7	1646.0	129.0		0.4	0.3	6.9	9.8		0.08
12	30.3	30.1	1242.0	129.0			0.7	3.4	13.7			0.15
13	51.8	84.4	326.7	480.9			0.6	5.2	16.1			0.12
14	33.7	100.0	378.0				0.6	6.2				0.08
15	161.0	72.3	159.0	476.0			0.6	1.9	5.0			0.06
16	25.9	47.8	267.0	1042.0			0.6	3.8	12.7			0.15
17	28.1	222.0	1323.0				1.2	8.7				0.08
18	159.0	144.0	723.0	83.7			1.5	7.1	27.5			0.10
19	89.8	40.3	1442.0	14.6			3.5	1.6	29.7			0.10
20	141.9	53.2	618.3	202.3			0.3	3.1	23.2			0.10
21	61.7	59.3	1158.0	159.0			3.6	0.3	26.5			0.09
22	59.8	191.0	1180.0	46.1			0.9	8.4	25.8			0.08
23	86.3	336.0	1060.0	202.0			4.8	3.0	16.2			0.08
24	90.9	302.0	621.0				4.8	13.9				0.10
25	208.1	439.5	1145.0	107.9	2811.0		0.8	7.1	13.0	21.6		0.23

Table 2. Geoelectric parameters obtained from the analysis of the VES measurements (continued)

VES Location	Resistivity (ohm-m)						Depth (m)					Longitudinal Conductance
	ρ1	ρ2	ρ3	ρ4	ρ5	ρ6	h1	h2	h3	h4	h5	(mho)
26	44.4	251.0	1549.0	163.0			1.1	13.7	37.0			0.10
27	46.5	133.0	496.0	1265.0			0.3	3.3	58.3			0.15
28	36.9	85.8	695.0	1009.0			0.8	4.9	15.3			0.10
29	124.0	186.0	984.0	202.0			0.6	8.4	37.1			0.09
30	40.3	113.0	591.0	1423.0	23.3		0.1	3.2	35.6	43.0		0.12
31	32.3	213.0	1945.0	217.0			0.5	3.9	30.6			0.05
32	49.6	233.0	1640.0	208.0			0.5	3.4	33.4			0.05
33	75.5	390.0	2387.0	570.0			2.5	5.3	9.8			0.05
34	54.5	260.0	2644.0	501.0			0.7	6.1	9.1			0.04
35	89.7	375.0	885.0				1.4	17.7				0.06
36	33.7	61.5	1000.0				0.5	6.5				0.12
37	13.6	37.8	3244.0	194.0			0.1	4.9	28.3			0.15
38	250.0	31.6	1026.0	180.0			0.2	5.1	24.8			0.19
39	33.8	57.3	1053.0	258.0			1.3	6.3	29.3			0.18
40	128.0	54.1	251.0	1108.0	324.0		0.3	4.6	12.7	23.3		0.16

The model parameters obtained from the analysis of the VES measurements give insight into how the resistivity in the study area varies both laterally and vertically. This resistivity variation provides means by which the lithology of the subsurface was inferred. Generally, the model reveals that the subsurface lithology up to the depth of investigation can be represented with a three to four-layer model. The geology of the coastal plain sands of Lagos, which underlies the study area, is characterized by alternation of sand and clay, with the presence of lenses of clayey sand, sandy clay and silty clay in some places [25]. Similar lithology is observed in the borehole log (Figure 4). The lithological interpretation of the layers of the resistivity models was based on the geology of the area and the borehole log. An example of the interpretation of the resistivity model for VES location 9 is given in Table 3.

Table 3. Interpreted Resistivity Model for VES 9

Layer	Interpreted Geology	Resistivity (ohm-m)	Thickness(m)	Depth
1	Topsoil	135.0	1.3	0.6
2	Sandy Clay	413.0	1.6	8.6
3	Contaminated Unit	1668.0	17.1	26.5
4	Clayey Sand	79.4	-	-

3.1.1 Vertical distribution of geoelectric parameters

The vertical distribution of the geoelectric parameters is a 2-D pseudo geoelectric section of VES locations along a traverse. Seven geoelectric sections were generated, with the general model for the study area consisting of three to four layers of the following units - topsoil, contaminated unit, sandy clay/clayey unit. The thickness and occurrence of these units vary slightly across the study area. The geoelectric sections for Traverses 5, 1 and 2 trend generally from the northwest to the southeastern part of the study area (Figure 6a, b, c, respectively). Traverse 2 shows the highest resistivity for the contaminated second layer, while Traverse 5 has the greatest thickness. It is observed that the contaminated layer commences at almost the surface (at VES 25) on traverse 5, which indicates a probable contamination source. Traverses 4 (SW – NE) and 6 (NE –SW) are parallel to each other, and they both exhibit similar lithology (three to four lithologic units) ranging from topsoil, sandy clay/clayey sand, contaminated unit and sandy clay/clayey sand. The contaminated unit shows relatively high resistivity (up to 2644 ohm-m) in traverse 6, suggesting a greater level of contamination. The geoelectric section along traverse 3 is in the northeastern part of the study area and runs NE to SW. It shows three lithologies (Figure 6f), with the contaminated unit occurring at greater depths (average of 12 m) compared to the other traverses. Also, the resistivity of this unit shows a trend of increase towards the southwestern part of the section, which is in the direction of the location of the other traverses. Traverse 7 is located in the southern part of the study area and runs in the NW – SW direction. It also shows a three-four layer model, with the contaminated unit having resistivity that is relatively high (≥ 1000 ohm-m) across the section. This suggests a significant level of contamination from about 7 m in the NW end to 15 m in the SW end.

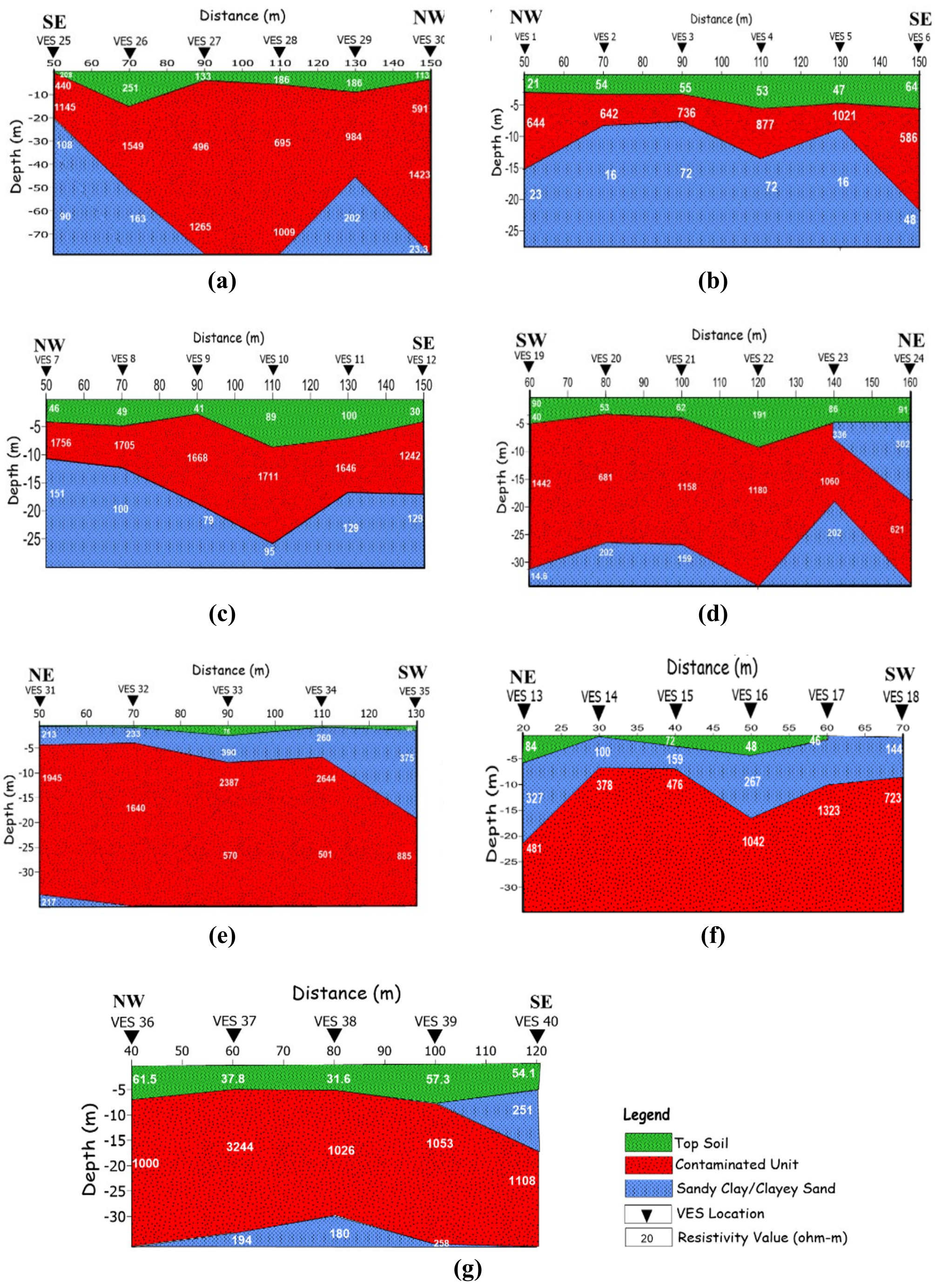

Figure 6. Geoelectric section along (a) Traverse 5 (b) Traverse 1 (c) Traverse 2 (d) Traverse 4 (e) Traverse 6 (f) Traverse 3 (g) Traverse 7

3.1.2 Longitudinal conductance and protective capacity

Longitudinal conductance (SL) calculated using the geoelectric parameters of the overburden layers (Equation 1) as obtained from the inversion of the 1D VES for each location is given in Table 2. The results indicate a variation in S_L ranging from 0.04 to 1.55. The average S_L for the study area is approximately 0.17, and according to Table 2, it indicates that the study area has weak/poor protective capacity. This also implies the subsurface is highly vulnerable to pollution, and the groundwater system is especially susceptible.

3.2 2D Electrical Resistivity Imaging (ERI)

Figure 7 shows the 2D ERI section for traverses 1, 2 and 5. These traverses run parallel to the orientation (NW – SE) of a known pipeline in the area. The resistivity model obtained indicates a three-layer lithology for all the traverses. The first zone is a low resistivity top layer (< 200 Ωm) that spans from about 0-10 m from the surface, followed by a high resistivity zone (> 400 Ωm) that generally commences from about 5-30 m below the surface. Below this zone is a low resistivity zone of < 221 ohm- m commencing from a depth of about 30 m below the surface. The lithology sequence varies in thickness and resistivity value across the traverses, indicating a possible variation in the lithology and/or resistivity of the saturating fluid. However, it is observed that the resistivity value for the second zone for traverse 5 is relatively low compared to the other traverses (Figure 7c). Also, a unique linear feature from line position of about 60 m to 100 m, with a resistivity value less than 300 Ωm from the surface to the bottom of the section (30m), is observed. This has been interpreted as a possible fault structure. Another important feature observed on traverse five occurs at line positions 30 m and 60 m, where the second zone with higher resistivity (> 400 Ωm) was observed to commence from the surface, implying the contamination of that region by a conducting fluid, i.e. a leak from the pipeline.

The 2D ERI section for traverses 6 and 4 is shown in Figure 8. Both traverses run parallel to each other and intersect traverse 5 at different points (see Figure 3). A similar three lithology layers can be inferred as obtained in the previous traverses, down to a depth of about 35 m. However, traverse 6 (Figure 8a) shows relatively high resistivity in the second layer than traverse 4 (Figure 8b), suggesting a higher degree of contamination. Traverse 3 (Figure 8c) has a total spread of 100 m, and an electrode spacing of 5 m was used due to spacing constraints. The depth of resolution of the 2D ERI for this traverse is 15m; however, it can be observed that the resolution of the upper layers is well defined and the depth to the zone of high resistivity (> 500 Ωm) occurs at about 12 m. Also, around line position 80 m, a zone of high resistivity (> 345 Ωm) is observed from the surface. Such an anomaly signature has been classified as probably being due to leakage from the pipeline.

Traverse 7 was initially identified as a possible control for the study, but it was observed that water from wells close to VES 36 on the traverse had a strong hydrocarbon smell, which was suggestive of contamination of the aquifer unit. The 2D section (Figure 9a) shows similar lithology to the other traverses, however the resistivity values obtained for the second layer (> 500 Ωm, but < 1500 Ωm) still suggest possible significant levels of contamination.

As a comparison, the ERI sections obtained from locations having similar subsurface geology (see Figure 10) and known to be free from any hydrocarbon contamination are shown in Figure 9b and Figure 9c. The general trend of the resistivity values down to a depth of about 35 m is relatively lower (< 350 ohm-m) than that for the study area. This supports the argument that the anomalous high resistivity observed in the second layer (between 15-35 m depth) can be attributed to groundwater infiltration with hydrocarbons [26].

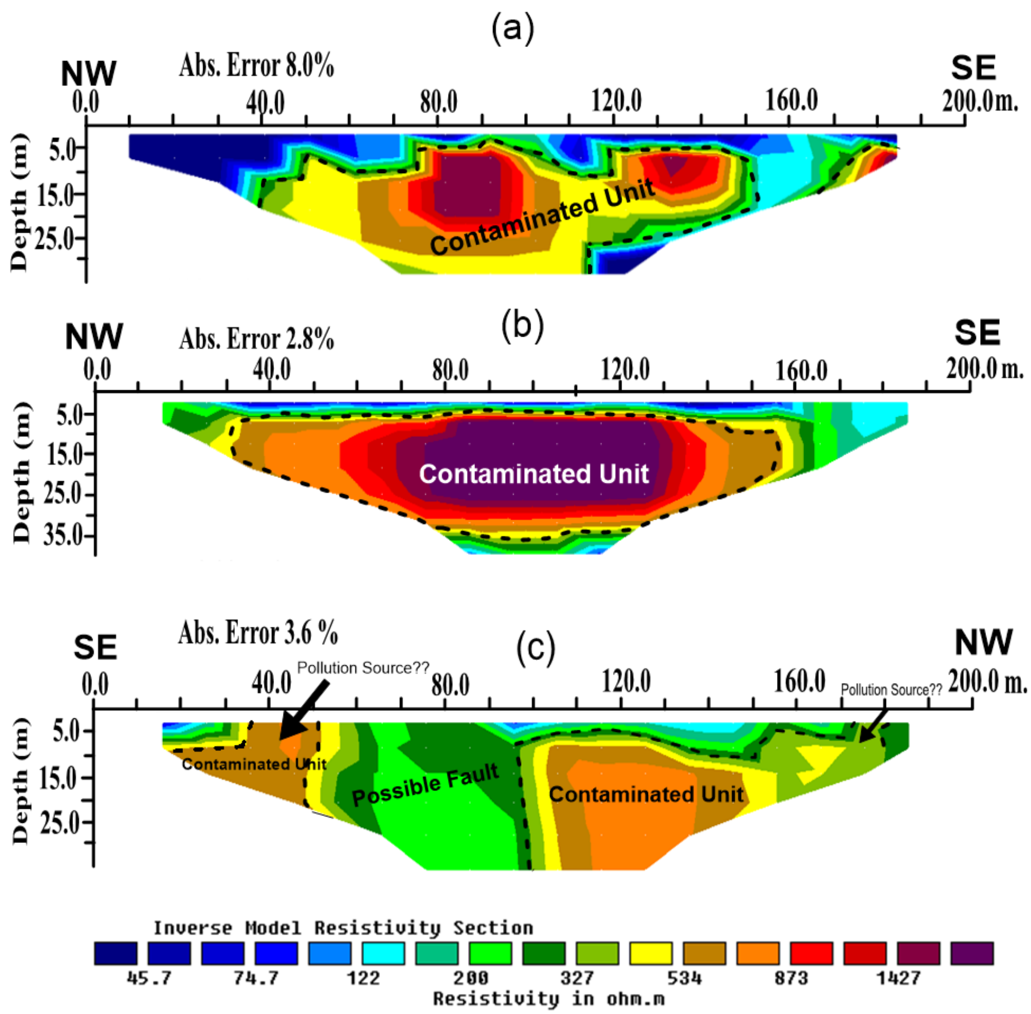

Figure 7. Inverted resistivity section obtained from the analysis of the 2D ERI measurements along (a) Traverse one, (b) Traverse two, and (c) Traverse five

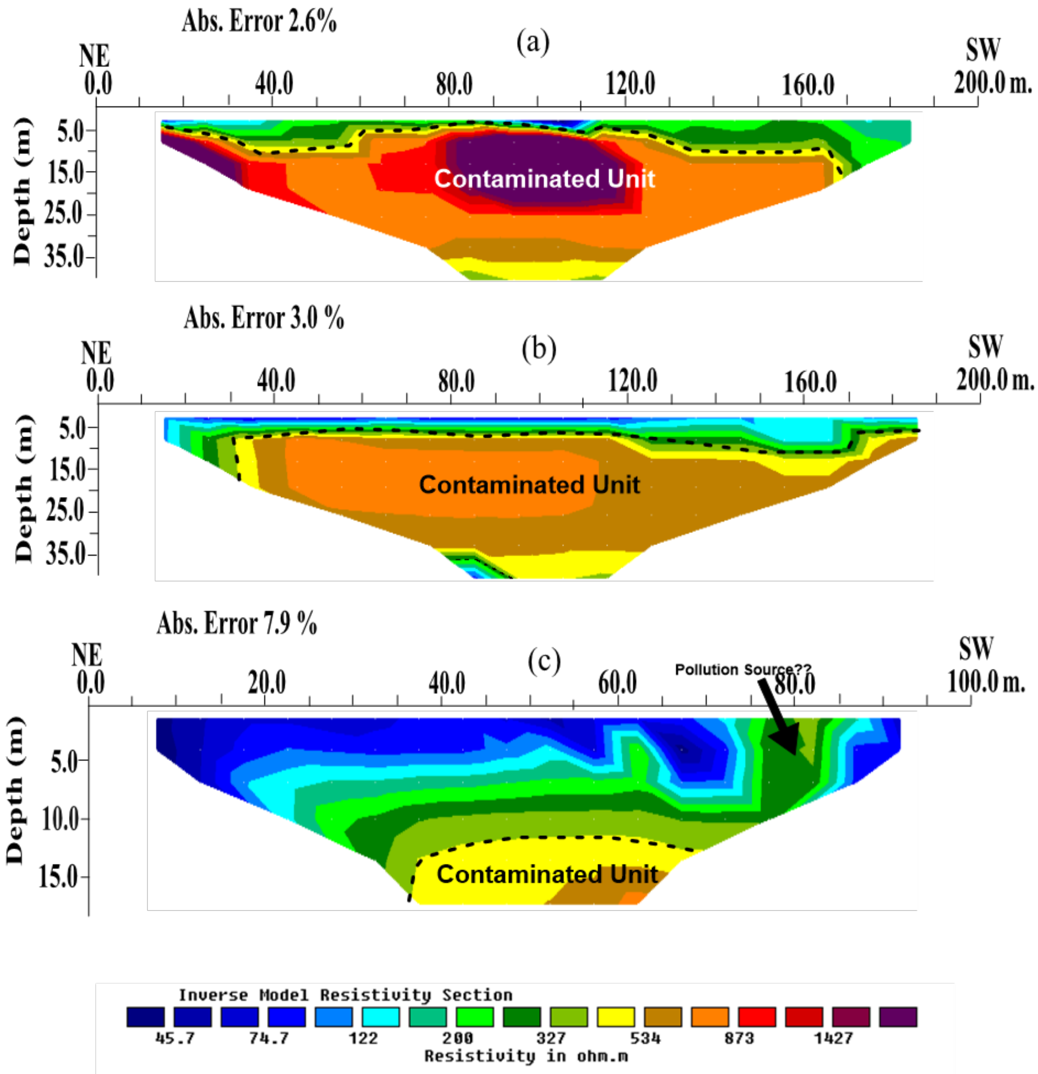

Figure 8. Inverted resistivity section obtained from the analysis of the 2D ERI measurements along (a) Traverse 6, (b) Traverse 4, and (c) Traverse 3

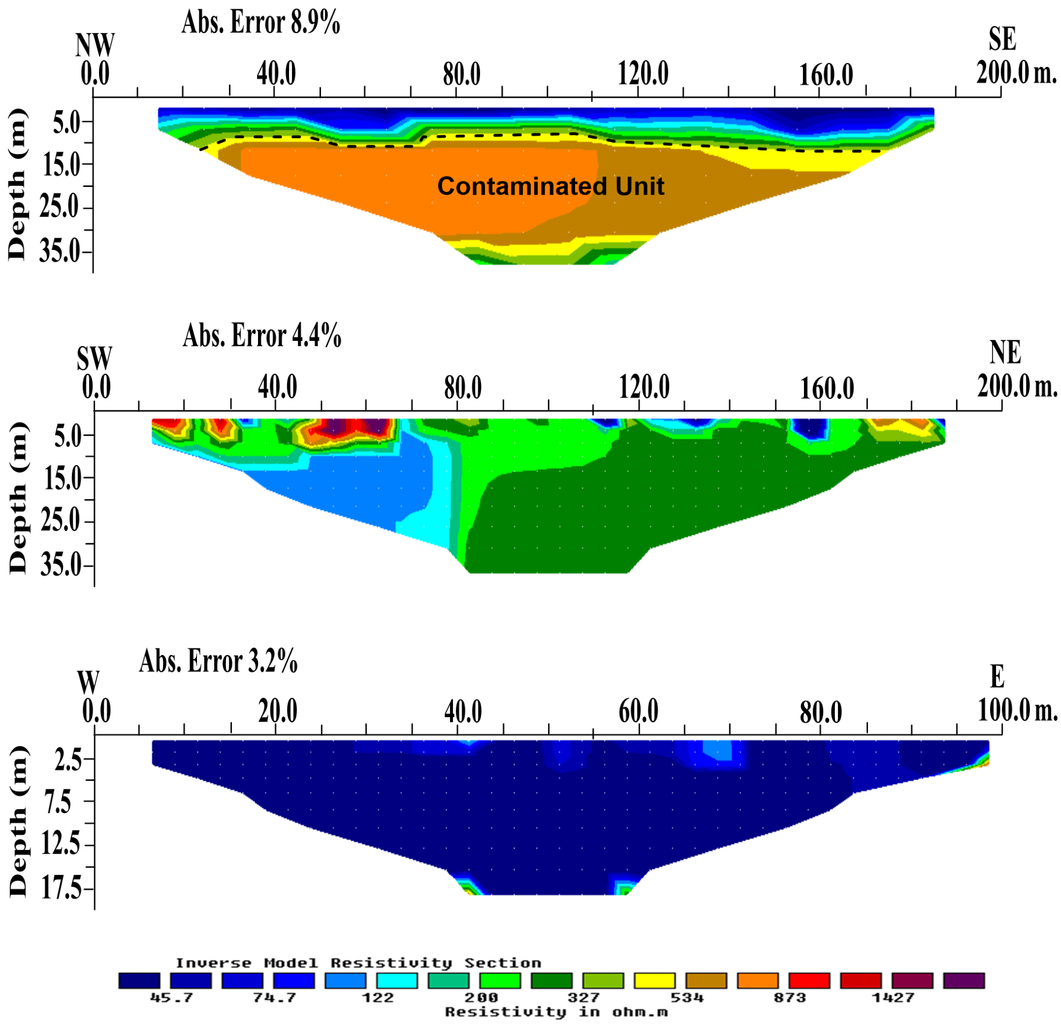

Figure 9. Inverted resistivity section obtained from the analysis of the 2D ERI measurements along (a) Traverse seven, (b) Control traverse 1, and (c) Control traverse 2

A broad characterization of the subsurface as obtained from the 2D ERI results shows that the first layer is characterized with low resistivity materials (6-200 Ωm) and at a depth ranging from about 2 to 10m. This is interpreted as being the topsoil material. The second layer shows a relatively higher resistivity (> 400 Ωm) commencing from a depth of about 10 to 35 m, which coincides with the expected aquiferous unit of the area. The aquifers in the coastal plain sands are an important source of groundwater in the study area and are mostly exploited using hand-dug wells and or manually drilled boreholes [16, 27]. The shallow aquifer occurs at a depth range of 5 to 32 m [15, 28] and it coincides with the depth of hand-dug wells and domestically drilled boreholes in the study area. A correlation with the borehole log (Figure 4) suggests this unit is characterized by laterite, reddish sandy clay and whitish sandy clay. Although several authors have reported the resistivity values of saturated units to be less than 200 ohm-m [27, 29], it is expected that hydrocarbon contamination of this layer would result in an increase in resistivity [30].

It is worthy of note that all the traverses in the study area exhibit this high resistivity intermediate layer, although with varying resistivity. Reports from residents indicate that the contamination of their wells (aquifer) usually commences with the incidence of hydrocarbon odor detected in the water, after which the water drawn from the wells becomes mixed with hydrocarbon. In some cases, the mixture consists of a significant level of crude oil [13]. This variation in the level of contamination could probably be the result of the variation in the resistivity range (400 to 5,000 Ωm).

The third layer shows a lower resistivity value, generally less than 220 Ωm, which has been inferred as being characteristic of clay/sandy clay.

In Figure 10, traverses 1, 2, 4, 5 and 6 were overlain to provide an idea of the flow direction. The high resistivity (> 400 ohm-m) contaminated second layer is present in all the sections. The hydrocarbon migration from the location of the spillage is usually down the soil column and accumulates as a lens above the water table [31]. This is observed in the ERI section as the high resistivity value which goes from the surface downwards (locations marked as possible pollution source on Figure 10). At the same time, locations of very high resistivity lenses are also observed which are an indication of an accumulation of hydrocarbons. In general, the flow direction of the pollution is a function of different factors such as groundwater level and hydraulic gradient, which have not been determined in this study. The results, however, shows that the contamination is wide spread in the area.

(a)

(b)

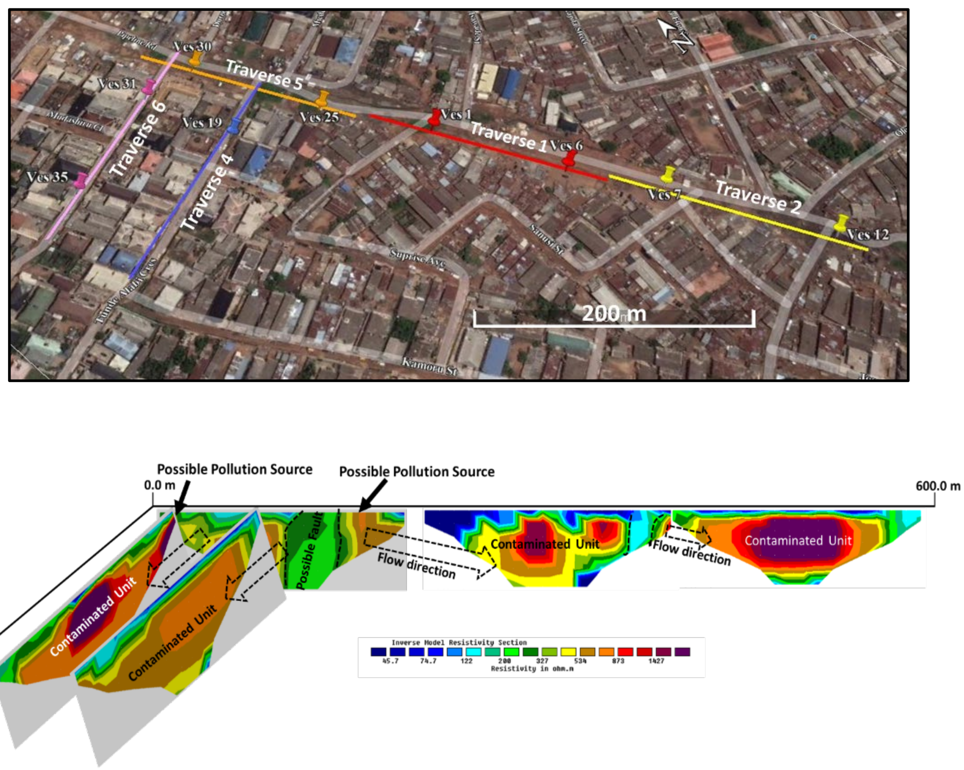

Figure 10. (a) Google earth image showing traverses 1, 2, 5, 4 and 6, (b) 2D ERI section for traverses 1, 2, 5, 4 and 6 showing the flow direction of the hydrocarbon contaminant

4. Conclusions

In general, the subsurface model for the study area can be characterised by three distinct geoelectric layers to a depth of about 50 m. These layers correspond to the topsoil (clay, clayey sand), lateritic/sandy clay (which is saturated – possibly contaminated with hydrocarbon in most cases) and a bottom layer composed of sandy clay/clay. The relatively high resistivity obtained for the second layer suggests that this layer has been contaminated with hydrocarbons, and it occurs from a depth of about 5 m to 35 m. This coincides with the depth of the shallow aquifer that serves as the main source of potable water for the inhabitants of the area. The degree of contamination differs across the study area; however, results from the longitudinal conductance shows slight variation in the vulnerability of the subsurface layers to contamination. In general, the study area is extremely vulnerable to pollution given the average S_L obtained which is 0.04. Considering the pollution of the shallow aquifer, it is expected that the other aquifer units at depths greater than 35 m can be exploited for groundwater. However, it is important that the drilling of such wells should be regulated to ensure that the groundwater system is optimally managed. The 2D ERI models enabled the identification of anomalous features such as the locations of possible leakages. These were identified as anomalously high resistivity signatures observed from the surface of the ERI traverses 3 and 5. The identification of the location of possible leakages of the pipeline can help the relevant authorities design and implement mitigation measures to prevent pollution. Also, a linear resistivity feature is clearly observed on traverse 5, which seems to truncate the flow of the hydrocarbon contamination unit across the traverse. More investigation is needed to effectively characterize this feature.

This study has highlighted the effectiveness of the electrical resistivity methods in identifying and mapping hydrocarbon pollution in Ejigbo area of Lagos states. In particular, the utilization of the 2D ERI method has been more effective in this regard, as it gives a better subsurface image and allows for an identification of possible locations of spillage. Although the 1D VES is an easy and fast means of obtaining information from the subsurface, the resolution in terms of mapping and identifying hydrocarbon contamination is greatly affected by its resolution and solution non-uniqueness. However, the utilization of both VES and 2D ERI data is useful in constraining data inversion, and has ensured the development of a more robust model of the subsurface.

5. Acknowledgements

The authors appreciate the support of the Earth Signature Research Group of the University of Lagos. Also, we appreciate the help of Mr. Mohammed Hassan Bello of Hydro Bee Civil and Water Nigeria Limited for providing the borehole log utilized for this study. The anonymous reviewers are also greatly appreciated for the comments which greatly improved the work.

References

[1] Mekonnen, M.M. and Hoekstra, A.Y., 2016. Four billion people facing severe water scarcity. *Science Advances*, 2(2), DOI: 10.1126/sciadv.1500323.

[2] Aroh, K.N., Ubong, I.U., Eze, C.L., Harry, I.M., Umo-Otong, J.C. and Gobo, A.E., 2010. Oil spill incidents and pipeline vandalization in Nigeria: Impact on public health and negation to attainment of Millennium development goal: the Ishiagu example. *Disaster Prevention and Management*, 19(1), 70-87.

[3] Ossai, I.C., Ahmed, A., Hassan, A. and Hamid, F.S., 2020. Remediation of soil and water contaminated with petroleum hydrocarbon: A review. *Environmental Technology and Innovation*, 17, DOI: 10.1016/j.eti.2019.100526.

[4] Adeniji, A.E., Omonona, O.V., Obiora, D.N. and Chukudebelu, J.U., 2014. Evaluation of soil corrosivity and aquifer protective capacity using geoelectrical investigation in Bwari basement complex area, Abuja. *Journal of Earth System Science*, 123(3), 491-502.

[5] George, N.J., Nathaniel, E.U. and Etuk, S.E., 2014. Assessment of economically accessible groundwater reserve and its protective capacity in Eastern Obolo local government area of Akwa Ibom State, Nigeria, using electrical resistivity method. *International Scholarly Research Notices Geophysics*, 2014, DOI: 10.1155/2014/578981.

[6] Azhar, M.A., Suryadi, A., Samsudin, A.R., Yaacob, W.Z.W. and Saidin, A.N., 2016. 2D Geo-electrical resistivity imaging (ERI) of hydrocarbon contaminated soil. *Electronic Journal of Geotechnical Engineering*, 21, 299-304.

[7] Burazer, M. and Bowen, M.S., 2012. Geo electrical signature of long term hydrocarbon contamination in Serbia. *International Journal of Science and Research*, 3, 942-949.

[8] Aranda, R.M.R., Pagán, P.M. and Cano, A.F., 2012. Methodology for the detection of contamination by hydrocarbons and further soil sampling for volatile and semi-volatile organic enrichment in former petrol stations, SE Spain. *Eurasian Journal of Soil Science*, 1(1), 10-15.

[9] Delgado-Rodríguez, O., Shevnin, V., Peinado-Guevara, H. and de Guevara-Torres, M.L., 2018. Characterization of hydrocarbon-contaminated sites based on geoelectrical methods of geophysical exploration. In: A. Okiwelu, ed. *Geophysics*. London: InTechOpen, pp. 85-93.

[10] Fatoba, J.O., Omolayo, S.D., and Adigun, E.O., 2014. Using geoelectric soundings for estimation of hydraulic characteristics of aquifers in the coastal area of Lagos, Southwestern Nigeria. *International Letters of Natural Sciences*, 11, 30-39.

[11] Adeoti, L., Bello, M.A., Olatinsu, O.B. and Adiat, K.A.N., 2015. Application of geoelectrical and chemical methods for groundwater assessment in Isheri-North, Ogun state, Nigeria. *Journal of Science and Technology (Ghana)*, 35(1), 24-38.

[12] Obiora, D.N. and Ibuot, J.C., 2020. Geophysical assessment of aquifer vulnerability and management: a case study of University of Nigeria, Nsukka, Enugu State. *Applied Water Science*, 10(1), 1-11, DOI: 10.2478/ast-2021-0001.

[13] Folarin, S., 2020. Killing Them Softly: A Lagos Community Where Residence Drank and Bath with Petrol Water. [online] Available at: https://punchng.com/killing-them-softly-a-lagos-community-where-residents-drink-bathe-with-petrol-water.

[14] Olabode, S.O. and Mohammed, M.Z., 2016. Depositional facies and sequence stratigraphic study in parts of Benin (Dahomey) basin SW Nigeria: Implications on the re-interpretation of tertiary sedimentary successions. *International Journal of Geosciences*, 7(2), 210-228.

[15] Yusuf, M.A., Abiye, T.A., Butler, M.J. and Ibrahim, K.O., 2018. Origin and residence time of shallow groundwater resources in Lagos coastal basin, south-west Nigeria: An isotopic approach. *Heliyon*, 4(11), DOI: 10.1016/j.heliyon.2018.e00932.

[16] Healy, A., Upton, K., Capstick, S., Bristow, G., Tijani, M., MacDonald, A., Goni, I., Bukar, Y., Whitmarsh, L., Theis, S. and Danert, K., 2020. Domestic groundwater abstraction in Lagos, Nigeria: a disjuncture in the science-policy-practice interface? *Environmental Research Letters*, 15(4), DOI: 10.1088/1748-9326/ab7463.

[17] Nigerian Geological Survey Agency, 2020. *Geological Maps*. [online] Available at: http://ngsa.gov.ng/geological-maps.

[18] Loke, M.H., 2002. *Tutorial: 2-D and 3-D Electrical Imaging Surveys*. [online] Available at: http://personales.upv.es/jpadin/coursenotes.pdf.

[19] Loke, M.H. and Barker, R.D., 1996. Rapid least - squares inversion of apparent resistivity pseudosections by a quasi - Newton method 1. *Geophysical Prospecting*, 44(1), 131-152.
[20] Greggio, N., Giambastiani, B., Balugani, E., Amaini, C. and Antonellini, M., 2018. High-resolution electrical resistivity tomography (ERT) to characterize the spatial extension of freshwater lenses in a salinized coastal aquifer. *Water*, 10(8), DOI: 10.3390/ w10081067.
[21] Adeoti, L., Oladele, S. and Ogunlana, F., 2011. Geo-electrical investigation of leachate impact on groundwater: A case study of Ile-Epo dumpsite, Lagos, Nigeria. *Journal of Applied Sciences and Environmental Management,* 15(2), 361-364.
[22] Shailaja, G., Laxminarayana, M., Patil, J.D., Erram, V.C., Suryawanshi, R.A. and Gupta, G., 2016. Efficacy of anisotropic properties in groundwater exploration from geoelectric sounding over trap covered terrain. *Journal of Indian Geophysical Union*, 20(5), 453-461.
[23] Oladapo, M.I., Mohammed, M.Z., Adeoye, O.O. and Adetola, B.A., 2004. Geoelectrical investigation of the Ondo state housing corporation estate Ijapo Akure, Southwestern Nigeria. *Journal of Mining and Geology*, 40(1), 41-48.
[24] Stempvoort, D.V., Ewert, L. and Wassenaar, L., 1993. Aquifer vulnerability index: a GIS-compatible method for groundwater vulnerability mapping. *Canadian Water Resources Journal,* 18(1), 25-37.
[25] Ilugbo, S.O., Edunjobi, H.O., Alabi, T.O., Ogabi, A.F., Olomo, K.O., Ojo, O.A. and Adeleke, K.A., 2019. Evaluation of groundwater level using combined electrical resistivity log with gamma (Elgg) around Ikeja, Lagos State, Southwestern Nigeria. *Asian Journal of Geological Research*, 2(3), 1-13.
[26] Raji, L., Obadare, I. and Odukoya, A.M., 2017. Geophysical evaluation of an oil-contaminated coastal environment, Lagos, Nigeria. *SEG International Exposition and 87th Annual Meeting*, Houston, USA, September 24-29, 2017, pp. 5412-5417.
[27] Ayolabi, E.A., Aluko, K., Raji, W. and Ayolabi, E., 2017. Application of 2-D resistivity survey to groundwater aquifer delineation in a sedimentary terrain: Application of 2-D resistivity survey to groundwater aquifer delineation in a sedimentary terrain: A case study of South-western Nigeria. *Water Utility Journal*, 17, 71-79.
[28] Oladapo, M.I., Ilori, O.B. and Adeoye-Oladapo, O.O., 2014. Geophysical study of saline water intrusion in Lagos municipality. *African Journal of Environmental Science and Technology*, 8(1), 16-30.
[29] Osinowo, O.O. and Olayinka, A.I., 2012. Very low frequency electromagnetic (VLF-EM) and electrical resistivity (ER) investigation for groundwater potential evaluation in a complex geological terrain around the Ijebu-Ode transition zone, southwestern Nigeria. *Journal of Geophysics and Engineering*, 9(4), 374-396.
[30] Oyinkuro, O.A. and Wariebi, K.A., 2017. Hydrocarbon spill site characterization by electrical resistivity tomography and ground penetrating radar methods - A review. *Asian Journal of Environment and Ecology,* 4(3), DOI: 10.9734/AJEE/2017/36742.
[31] Akinrinade, O.J. and Christopher, O., 2016. Geoelectric delineation of hydrocarbon spill in Abesan Lagos, Nigeria. *Journal of Emerging Trends in Engineering and Applied Sciences*, 7(1), 35-44.